Modeling of Switching Cores for Induction Accelerators

Henry D. Shay, John F. DeFord, George D. Craig
Lawrence Livermore National Laboratory
Livermore, CA 94550

Abstract

We have successfully installed a nonlinear magnetization model in the 2 1/2-D finite difference (FDTD) electro-magnetic (EM) code AMOS. We have developed a procedure for mapping the 3-D induction cells on the 2-D AMOS mesh. These tools will be important for modeling advanced induction accelerator cells.

I. INTRODUCTION

Many future applications of induction accelerators (IA) require high quality beams and, in particular, rather small variation in beam energy. For heavy ion fusion (HIF) beams it is necessary to have an energy variation less than 0.1% so that the beams can be focussed to a small enough spot on the fusion target.[1] One of the key components in determining the energy variation of an IA beam is the ferrite or Metglas core in an induction cell. The time dependent switching of these magnetic materials determines, in part, the variation of the cell gap voltage. In order to shorten the iteration time for design of and experiments on induction cells, there are several efforts to incorporate non-linear magnetization models in finite difference codes for calculating this time varying switching. One approach is to treatment the core as one or a few lumped variable inductors in a circuit model. This approach is surely appropriate for relatively small cores, but may not properly represent the passage of switching fronts in large cores. The induction cores for HIF require moderate to high gap voltages, often for several microseconds, and so require many volt-seconds. For example, an upper limit applied to linear induction accelerators for HIF is about 0.5 volt-seconds/m[2], and so, for a cell separation of less than about 5 m at the low energy end and a maximum magnetic field swing of 3 T, HIF cores can be as large as 1 m^2 and have dimensions which are a large fraction of a meter. We have, therefore, undertaken to install a non-linear constitutive model in a 2 1/2-D , FDTD EM code, AMOS. We describe in this paper the non-linear model, its incorporation in a 1-D test-bed, its incorporation in AMOS, and a technique for mapping 3-D geometries onto a 2-D calculational mesh.

II. 3-D GEOMETRY REPRESENTATION

Induction cell are driven with a small number of cable feeds, typically two, in a geometry which is intrinsically 3-D. AMOS uses a 2-D mesh. In order to calculate the switching of an induction cell, we developed a technique for representing the 3-D geometry in a 2-D axisymmetric mesh. We have represented the coaxial drive cables by a washer-shaped object spanning the region between the inner and outer radii of the core. Its conductivity was chosen so that its impedance matched the parallel impedance of coaxial drive cables (and related load matching resistors). We have tested whether such a washer would properly describe the scattering of axisymmetric waves (azimuthal mode number, m, of zero) by conducting calculations of scattering at the junction of three coaxial cables with two of the three cables zoned in the AMOS mesh and the third represented by a washer with an equivalent impedance. The analytic solution for the three coax junction is an elementary application of S-matrix theory, and AMOS correctly predicted both the transmitted and reflected waves. In the AMOS grid of the ETA II cell, we put a current source in the mock feed in order to provide an equivalent drive and were able to reproduce simultaneously the experimentally observed voltage and current histories of the ETA II cell.

III. NONLINEAR CONSTITUTIVE MODEL

M. Hodgdon [3] has developed an empirical nonlinear constitutive model, whose equations appear below:

$$\mu^{-1} = \alpha\,\mathrm{sign}(B)\left[f(B) - \dot{H}\right] + g\left(B,\dot{B}\right) \tag{1}$$

$$f(B) = \begin{cases} A_1\tan^P(A_2B) + A_5B & \text{for } |B| \le B_{bp} \\ A_1\tan^P(A_2B_{bp}) + A_5B_{bp} + (B - B_{bp})/\mu_s & \text{for } B > B_{bp} \\ -A_1\tan^P(A_2B_{bp}) - A_5B_{bp} + (B + B_{bp})/\mu_s & \text{for } B < -B_{bp} \end{cases} \tag{2}$$

$$g\left(B,\dot{B}\right) = \begin{cases} f'(B)\left[1 - A_3c\left(\dot{B}\right)\exp\left(-\dfrac{A_4|B|}{B_{cl} - |B|}\right)\right] & \text{for } |B| < B_{cl} \\ f'(B) & \text{otherwise} \end{cases} \tag{3}$$

$$c\left(\dot{B}\right) = \begin{cases} 1 + c_1|B| & \text{for } |\dot{B}| < \dot{B}_1 \\ 1 + c_1|B_1| + c_2\left(|\dot{B}| - |B_1|\right) & \text{for } |\dot{B}| > \dot{B}_1 \end{cases} \tag{4}$$

The permeability, μ, is a function of B, H, $\dot{B}$, and the direction of the traversal of the hystersis loop, that is, the sign of $\dot{B}$. This formulation permits the consideration of major and

Work performed under the auspices of the U.S.DOE by LLNL under W-7405-ENG-48

minor hysteresis loops. The function "f" is the inverse of the anhysteretic curve, and P, A_1, A_2, and A_5 are its fitting parameters. For |B| beyond B_{bp}, the slope of f is simply the saturation permeability of the Metglas, μ_S. As |B| approaches B_{cl}, the two halves of a hysteresis loop close at a rate determined by A_4. For |B| greater than B_{cl}, the two loops are merged. In typical parameterizations, B_{cl} and B_{bp} are nearly equal. For the DC hysteresis loop, $\dot{B}$ is zero, c is 1.0, and the width of the loop, twice the coercitivy, H_c, is determined just by the parameter A_3. For a pulsed hysteresis loop, $\dot{B}$ is not zero, and the width of the loop is c times the width of the DC loop. For most of the ferrites and Metglas under consideration, we have used piece-wise linear fits for c as a function of $\dot{B}$.

IV. 1-D FDTD Solution to Maxwell's Equations

Before installing this constitutive model into AMOS, we first tested it in a one 1-D test-bed. The test-bed used equations numbered (5), (6), and (7), which advance Maxwell's equations in a leap-frog scheme[4], and are substantially the same difference equations as those in AMOS. In the test-bed, we considered only the components E_x, B_y, and H_y.

$$\frac{B_{i+\frac{1}{2}}^{k+\frac{1}{2}} - B_{i+\frac{1}{2}}^{k-\frac{1}{2}}}{\Delta t} = -\frac{E_{i+1}^{k} - E_i^{k}}{\Delta z} \equiv \dot{B}_i^{k+\frac{1}{2}} \qquad (5)$$

$$H_{i+\frac{1}{2}}^{k+\frac{1}{2}} - H_{i+\frac{1}{2}}^{k-\frac{1}{2}} = \sum_{j=1}^{n} \left[\frac{\frac{1}{n}\left(B_{i+\frac{1}{2}}^{k+\frac{1}{2}} - B_{i+\frac{1}{2}}^{k-\frac{1}{2}} \right)}{\mu\left(B_{i+\frac{1}{2}}^{k-\frac{1}{2}} + \frac{j}{n}\left\{ B_{i+\frac{1}{2}}^{k+\frac{1}{2}} - B_{i+\frac{1}{2}}^{k-\frac{1}{2}} \right\}, H_{i+\frac{1}{2}}^{k-\frac{1}{2}}, \dot{B}_{i+\frac{1}{2}}^{k+\frac{1}{2}} \right)} \right] \qquad (6)$$

$$\varepsilon\left(\frac{E_i^{k+1} - E_i^{k}}{\Delta t} \right) = \frac{H_{i+\frac{1}{2}}^{k+\frac{1}{2}} - H_{i-\frac{1}{2}}^{k+\frac{1}{2}}}{\Delta z} \qquad (7)$$

Propagation is in the z-direction. The time index is k, and the z -index is i. The time step, Δt, is selected to obey the Courant condition, that is, that $\Delta t < \Delta z \sqrt{\varepsilon\mu_0}$, where Δz is the zone size. In this treatment, B serves as the independent variable advancing H via the permeability given by the constitutive model, μ as a function of B, H, and $\dot{B}$. Eq. (6) provides for n steps of sub-cycling in advancing H over each dB step on the hysteresis curve. In this sub-cycling, $\dot{B}$ is approximated as constant. In the 1-D model, we treat the conductivity of the Metglas as zero.

In addition to the formulation of the constitutive model shown above, we also tried a formulation in which all derivatives are kept continuous at B_{bp} and B_{cl} by smoothly joining the halves of f and g above and below the critical points. We found that so long as we limited the value of μ to fall within the range μ_S to about $10^5\mu_0$, we could use the simpler formulation of equations (5), (6), and (7). The limit at the high end prevented infinite slopes in the hysteresis curve ("back-bending"), which could generate pernicious numerical instabilities. For permeabilities below the lower limit, the Courant criterion would be violated, and, again, the solution would become unstable.

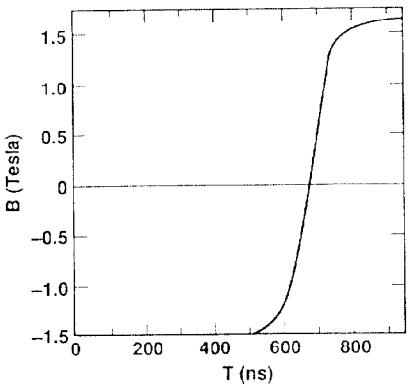

Figure 1 History of B in a thin sheet of Metglas as calculated in the 1-D test-bed.

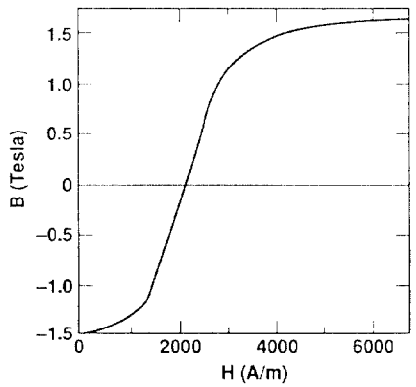

Figure 2 B-H curve for the 1D calculation of figure 1.

Sample results from 1-D test-bed calculations appear in figures 1 and 2. Both the plot of B versus time in figure 1 and the hysteresis switching curve of figure 2 have been taken from a calculation in which a plane wave impinged on a thin (1 cm) sheet of 2605SC Metglas. The right-hand-side (RHS) boundary conditions (BC) behind the Metglas sheet were those of a perfect conductor; we used a radiation BC on the LHS behind the source. The DC parameterization of the 2605SC Metglas is a modification of a parameterization provided by M. Hodgdon.[5] The c_i and $\dot{B}_i$ parameters describing the broadening of the hysteresis loop are taken from data of C. Smith of Allied Signal.[6] The two features in the model parameterizations which we were most careful to preserve were the magnetic induction at saturation and the variation of coercivity with $\dot{B}$. In this particular calculation, the sample was so small and the time scales so long that each of ten Metglas zones had nearly identical histories.

In the course of testing this magnetization model, we found that calculations with sub-cycling give virtually identical results to those without it. We therefore have not included sub-cycling in the implementation in AMOS. The use of the magnetization model did increase the running time, but not by

a prohibitive factor. Without the nonlinear model, the CPU time on an XMP CRAY spent per zone-time-step in a vectorized version of the code was 3.5μs. With the nonlinear model coded "inline" (that is, written in the same routine with differential equation solver rather than called as a subroutine - a procedure used to enable vectorization of the nonlinear model), the CPU time per zone-time-step was about 6 μs.

V. IMPLEMENTATION IN AMOS

The AMOS code is a 2 1/2-D EM simulator for use in the design of accelerator components.[7] It is 2 1/2-D in that it uses a 2-D r-z mesh, but assumes a harmonic variation of the fields in the azimuthal (ϕ) coordinate. The user specifies the azimuthal multipole number (m) at run time, and AMOS allows spatially varying materials and a variety of BC's that support component design.

The implementation of the nonlinear model in AMOS was nearly the same as shown in eq. (5), (6), and (7) except that we did not use sub-cycling. Only the azimuthal components of magnetic induction and intensity were linked by the nonlinear model. To represent the insulation between the layers of Metglas winding, we introduced an option for anisotropic conductivity such that the conductivity in the radial direction was zero and the conductivity in the azimuthal and axial directions could be independently chosen.

In the test problems we have so far conducted with this model in AMOS, we have examined exclusively the m=0 azimuthally symmetric mode. We have configured the Metglas as a large torus around a central conductor and bounded by conductors on the back, RHS boundary, and on the outer radius. On the LHS, we had a dielectric material. We placed a magnetic current source (an additional term in the **curl E** equation) on the LHS of the dielectric material and a radiation BC on its LHS. In this manner, any reflections from the Metglas propagating to the left could leave the mesh. In the particular calculation depicted in figures 3 and 4, the Metglas torus was 10 cm long and had an inner radius of 19 cm and an outer radius of 31 cm. The temporal history of the source was a Gaussian arising to a peak at 600 ns, at which time the calculation was terminated. Figure 3 shows the B-H curves for points at inner and outer radii on the LHS of the Metglas. Because the time derivative of the magnetic induction is smaller at the outer radius, that point has a lower coercivity than the point at smaller radius, but it was not driven as fully into saturation because of the lower peak H-field. This calculation was performed with zero conductivity in all directions, and so the Metglas could support a small axial electric field, as shown in figure 4. Because of the TEM_{00} nature of the drive, it excited neither radial nor axial components of magnetic induction. As expected, the radial electric field was much larger; it rose sharply during the period of large B, peaked as the Metglas began to enter saturation, and then began to fall.

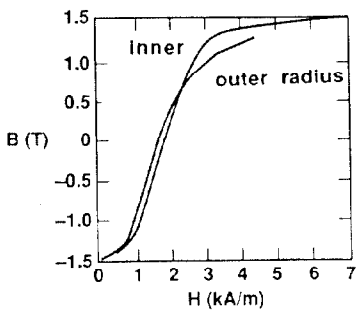

Figure 3. B-H curves from AMOS calculation of a Metglas torus

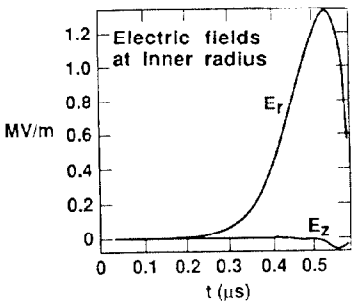

Figure 4. E fields from the AMOS calculation in figure 3.

VI. CONCLUSIONS

We have successfully installed a nonlinear magnetization model in the 2 1/2-D FDTD EM code AMOS. We have developed a procedure for mapping the 3-D induction cells on the 2-D AMOS mesh.

Future work will entail using this model for investigating several proposed HIF induction cells. We expect to install a simple vector analogue of the scalar magnetization model in AMOS and will latter implement it in a 3-D version of AMOS which is presently under development.

We gratefully acknowledge the help and advice given by M. L. Hodgdon, LANL, and C. H. Smith, Allied Signal.

REFERENCES

[1] J. Hovingh, V.O. Brady, A. Faltens, D. Keefe, and E. Lee, Fusion Technology, vol. 13, p. 255, 1988.

[2] C.H. Kim and L. Smith, "A Design Procedure for Acceleration and Bunching in an Ion Induction Linac," LBL-19137, 1985.

[3] M. L.Hodgdon, "Applications of a Theory of Ferromagnetic Hysteresis," IEEE Transactions on Magnetics, vol. 24, p. 218, 1988.

[4] K. Yee, "Numerical Solution of Initial Boundary Value Problems Involving Maxwell's Equations in Isotropic Media," IEEE Antennas and Propagation, vol. 14, p.302 , 1966.

[5] M. L. Hodgdon, private communication.

[6] C.H. Smith, "Applications of amorphous magnetic materials at very-high magnedtiztion rates," Journal of Applied Physics, vol. 67, p. 5556, 1990.

[7] J.F. DeFord, et al., "The AMOS Wakefield Code," Proceedings of the Conference on Computer Codes and the Linear Accelerator Community, Los Alamos National Laboratory, p. 265,1990.